Supporting Information

A Simplified Sum-Frequency Vibrational Imaging Setup Used for Imaging Lipid Bilayer Arrays

*Kathryn A. Smith and John C. Conboy**

Department of Chemistry, University of Utah, 315 S. 1400 E. RM. 2020, Salt Lake City, Utah 84112

Abstract:

The supporting information provides details about the materials and lipid bilayer preparation used in the manuscript. The supporting information also provides a detailed characterization of the lens-less sum-frequency imaging of a patterned asymmetric DSPC/DSPC-d_{70} lipid bilayer. Image analysis is used to characterize the propagation and diffraction properties of the systems which are discussed in terms of a Fraunhofer diffraction theory.

EXPERIMENTAL SECTION

Materials

DSPC, 1,2-distearoyl(d70)-*sn*-glycero-3-phosphocholine (DSPC-d_{70}), DOPC, DPPC and DMPC were obtained from Avanti Polar Lipids and used as received. Poly(allylamine hydrochloride) (PAH) (MW 56,000), HPLC grade Methanol and D_2O were purchased from Sigma-Aldrich. Sodium dodecyl sulfate (SDS) was purchased from Fisher Scientific. Spectroscopy grade $CHCl_3$ was obtained from EDM Millipore. Fused silica prisms (Almaz Optics) were used as the solid support for the PSLBs. The water used for bilayer preparation was obtained from a Nanopure Infinity Ultrapure water purification system (nanopure) with a minimum resistivity of 18.2 MΩ·cm.

Lipid Bilayer Preparation

The fused silica prisms were first cleaned in a freshly prepared piranha solution (70% sulfuric acid and 30% hydrogen peroxide) followed by rinsing with copious amounts of water. (*Caution!* Piranha is highly corrosive, reacting violently with organic solutions and materials and should be handled with care.) The substrate was then dried in an oven at 120°C for 20 minutes before Argon plasma cleaning (Harrick PDC-32G) for at least 3 minutes.

The asymmetric lipid bilayer was prepared using the Langmuir-Blodgett/Langmuir-Schaefer (LB/LS) method. A 1 mg/mL DSPC lipid solution in chloroform was deposited dropwise on the water subphase of a KSV Instrument Minitrough. The lipid layer was transferred onto a clean silica prism by pulling the substrate vertically out of the subphase at a surface pressure of 35 mN/m. The same prism was then passed horizontally into the subphase containing a monolayer of DSPC-d_{70} at 35 mN/m. The bilayer was then placed in a reservoir of water to be patterned using UV photolithography.

A fused silica positive 1951 United States Air Force (USAF) resolution test target (Edmund Optics) with a chrome pattern was used for UV photolithography. The USAF test target was placed in direct contact with the lipid bilayer and held in place with electrical tape. A pattern was generated by introducing UV light from a low pressure mercury vapor grid lamp ultra-violet ozone cleaner (Jelight Co.) for 13 minutes through the test target where the lipids not protected by the chrome pattern were etched away. The patterned bilayer was then assembled into a custom-built Teflon flow cell and then rinsed with D_2O. A thermistor (TE Technologies) inserted into the flow cell was used to monitor the temperature of the bulk solution. A circulating water bath (HAAKE Phoenix II P1, Thermo Fisher Scientific) was used to control the temperature of the flow cell. For the temperature scans, the temperature was increased rapidly (1~2°C/min) and followed by rapid cooling to room temperature.

Small Unilamellar Vesicle Preparation

Equal molar ratios of DOPC:DSPC, DOPC:DPPC and DMPC:DSPC as well as DOPC:DSPC plus 40 mol % cholesterol were premixed in chloroform, evaporated under a stream on N_2 (g) and placed under a vacuum overnight to remove any residual chloroform. The dried lipid film was incubated in phosphate buffer saline (PBS, pH 7.4, 140 mM NaCl, 10 mM KCl, 10 mM Na_2HPO_4, and 2 mM KH_2PO_4) at 65°C for at least 20 min. The lipid film was then resuspended by vortexing and sonication till clarity at 65°C. The final concentration of the small unilamellar vesicle (SUV) solution was 0.25 mg/mL.

MLBA Preparation

Details of the continuous flow microspotter (CFM) construction and MLBA preparation can be found elsewhere.[1,2] Briefly, a freshly cleaned silica prism was brought into contact with the PDMS printhead of the CFM to form a reversible seal. The printhead is a 5 x 12 mm^2 PDMS slab that has 48 spots of 400 x 400 μm^2 dimensions each connected to a pair of microchannels embedded within the PDMS plate. The SUV solutions were introduced individually into each microchannel at 65°C and circulated over the substrate for at least 30 min. The SUVs introduced under these conditions (elevated temperature and high salt concentration) will spontaneously fuse forming a symmetric bilayer.[3] Some microchannels circulated only PBS to serve as control spots. The SUV solutions were removed from the inlet wells and the microchannels were rinsed with PBS followed by nanopure while making sure the channels never completely emptied. The substrate was removed from the printhead in a reservoir of 1 mg/mL PAH solution and incubated for 20 min. The PAH electrostatically binds to any area of the bare silica surface not covered by PDMS residue, corralling the lipids on the surface preventing them from spreading.[4] The prism was then transferred to a water bath and assembled into a custom built flow cell. The flow cell was rinsed with D_2O before imaging. For the temperature scans, the temperature was brought up to 36°C at a rate of 0.3°C/min and then continued to heat and cool at a rate of 0.75°C/min.

RESULTS AND DISCUSSION

Lens-less SFVI

For this study, a simplified imaging system was sought to reduce the loss of photons traveling through unnecessary optics traditionally used in microscopy. For example, traditional microscopy experiments (i.e. fluorescence) produce incoherent light of many frequencies and phases in random directions and are characterized by a large divergence from the point source of

emission. Photons emanating from such point sources, like those generated in fluorescence, require the use of an objective to reconstruct the image. In contrast, SFG is a coherent process, meaning the generated photons are of the same frequency, phase and direction producing plane wave fronts (i.e. a monochromatic wave having the same value across a plane perpendicular to the direction of propagation) the collection of an image without the aid of a microscope should be possible, as long as the objects being imaged are several order of magnitude larger than the wavelength of light they emit.[5] Sly and co-workers have already shown the feasibility of lens-less imaging using second harmonic generation (SHG), a special case of SFG.[6] They were able to collect images of (S)-(+)-1,1'-bi-2-naphthol (SBN) binding to a patterned lipid bilayer using only filters to remove the fundamental light and a CCD for image collection when the detector was placed within the confocal distance of the emitted light from the surface.[6]

Lens-less images were collected using a patterned symmetric DSPC/DSPC-d_{70} lipid bilayer having three different sized pattern lines (397, 350 and 314 μm) at increasing distances from the sample stage to characterize the propagating sum-frequency beam. The white light images of the USAF test target group-element 0-3, 0-4 and 0-5 with corresponding line-widths of 397, 355 and 314 μm, respectively, used to pattern the lipid bilayer are shown in Figure S-1a. The asymmetric DSPC/DSPC-d_{70} lipid bilayer was selectively etched using ozone, to produce the negative of the test pattern shown in Figure S-1b. The SFVI images for each group-element presented in Figure S-1b were acquired with the CCD camera placed 12 cm away from the sample stage with the ω_{IR} tuned to 2875 cm^{-1} corresponding to the CH_3 ν_s. It should be noted that this distance was much shorter than the confocal distance of the setup. The confocal distance is the point at which the coherent beam is no longer collimated, diverging linearly with distance and the wave front

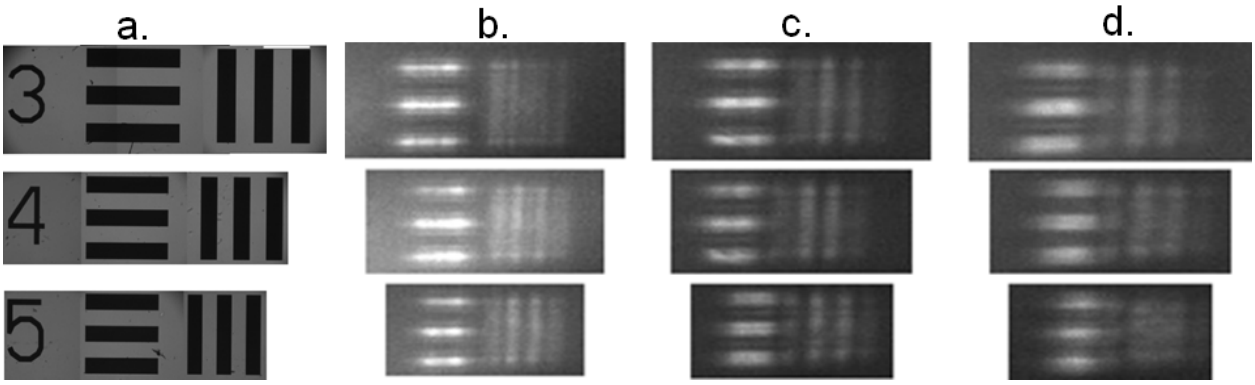

Figure S-1. (a) The white light image of the USAF test target for group-elements 0-3, 0-4 and 0-5 corresponding to the line-widths of 397, 355 and 314 μm, respectively. (b-d) The lens-less SFVI image of the DSPC/DSPC-d_{70} patterned bilayers prepared using the line-widths shown in (a) and acquired at 2875 cm^{-1}. The lens-less SFVI images were acquired at increasing distances from the sample stage at (b) 12, (c) 20 and (d) 26 cm.

become more spherical. Assuming a Gaussian beam profile, the confocal distance (z) can be defined as follows:[7]

$$z = \frac{\pi w_0^2}{\lambda} \qquad (1)$$

where λ is the wavelength of the beam and the spot size *w* defined as the full width at half maximum (FWHM). The confocal distance was calculated to be 67, 86 and 107 cm for the 314, 355 and 397 μm lines, respectively. The SFVI images in Figure S-1b show distorted images for all the different line-widths. The vertical lines remain unresolved for the group-elements 0-3 and 0-4 while four blurred vertical lines appear for the 0-5 group-element. While all the horizontal lines remain resolved from one another there exists a non-uniform intensity in both x and y directions with little resemblance to the rectangles shown in the USAF test target. Images were acquired at increasing distances from the substrate to further characterize the propagating SFG beam (Figure S-1c-d). At 20 cm the lines begin to look more uniform especially for the smaller 0-5 group-element until 26 cm where the images start to blur especially for the 0-5 group-element. This behavior is indicative of diffraction of the emitted SF light from the surface.

In order to verify diffraction was indeed causing the distortions measured in the SFVI images shown in Figure S-1, the line profiles obtained from the horizontal lines were compared to Fraunhofer diffraction theory[8]

$$I = I_0 \left(\frac{\sin\beta}{\beta}\right)^2 \qquad (2)$$

where $\beta = \frac{1}{2}ka \sin\theta$ with θ defined as the angle of the diffracted rays and *a* being the width of the slit and $k = 2\pi/\lambda$ where λ is the wavelength of light. The Franuhofer or far-field diffraction equation was used as the objects being measured were much larger than the wavelength of light emitted (~461 nm) and the emitted light is essentially a plane wave. Equation 2 was used to plot the intensity distribution from each line-width which was first normalized to the primary peaks at

the appropriate distances of the plot profiles obtained from the SFVI images. The three individual intensity distributions obtained from Equation 2 were summed together to obtain the intensity profiles plotted in Figure S-2. Examination of Figure S-2, reveals that the Fraunhofer diffraction (grey lines) correlates extremely well with the intensity distribution measured from the SFVI images (black lines). At close distances (12 cm) the calculated and measured intensity distributions both show that the principal maximums have narrower line widths than the USAF test pattern. The lower intensity diffraction peaks observed in the SFVI images, which decrease rapidly off the principal maximum, line up reasonably well with the higher order diffraction peaks predicted by theory. As the distance is increased between the detector and sample the higher order diffraction peaks are not readily resolved in the SFVI images and the line-widths begin to broaden. This again is predicted by the diffraction theory which shows the widening of the line-widths and disappearance of the higher order diffraction maxima.

The observation of such prominent diffraction was somewhat surprising, as diffraction was not observed in the SHG experiment performed by Sly et al. at distances shorter than the confocal distance for the same line-widths.[6] However, a counter-propagating geometry was used in the SHG experiment in which, the SHG beam is emitted normal to the surface. In the SFVI experiments performed here, using a total internal reflection geometry, the SFG beam cannot be generated normal to the surface even in a counter-propagating geometry because of the vastly different frequencies of the two input beams. As a result, the resultant SFG beam is being radiated at an angle close to 67° rendering lens-less imaging impractical because interference occurs between adjacent wave fronts.

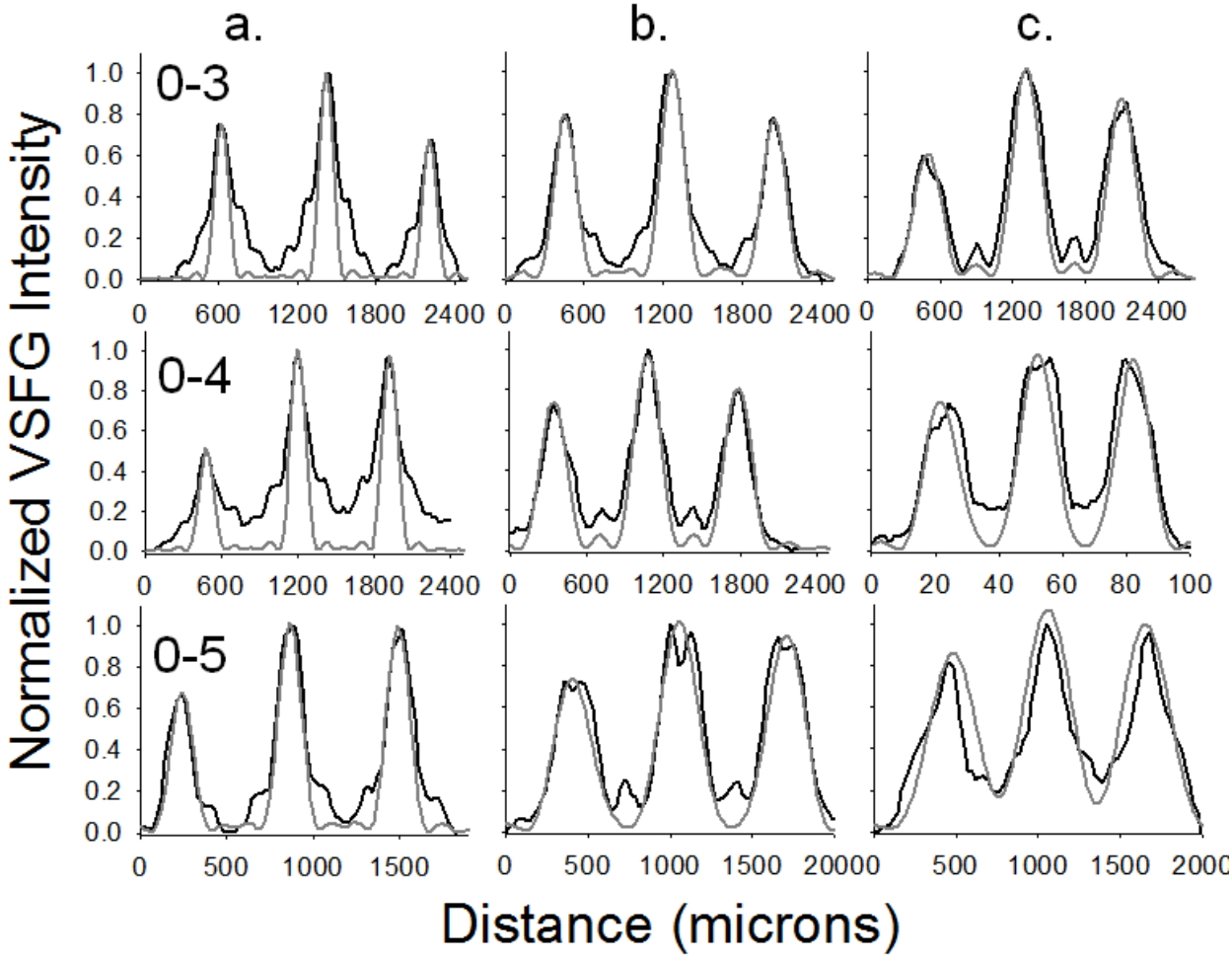

Figure S-2. (a) The intensity plot profiles for the horizontal lines in Figure S-1b are show by the black solid lines as a function of object-detector distance (a) 12, (b) 20 and (c) 26 cm. The grey lines represent the theoretical diffraction pattern produce by the respective line-widths from Equation 2.

REFERENCES

(1) Chang-Yen, D. A.; Myszka, D. G.; Gale, B. K. *Journal of Microelectromechanical Systems* **2006**, *15*, 1145.

(2) Smith, K. A.; Gale, B. K.; Conboy, J. C. *Analytical Chemistry (Washington, DC, United States)* **2008**, *80*, 7980.

(3) Wacklin, H. P. *Langmuir* **2011**, *27*, 7698.

(4) Burridge, K. A.; Figa, M. A.; Wong, J. Y. *Langmuir* **2004**, *20*, 10252.

(5) Milonni, P. W.; Eberly, J. H. *Lasers*; John Wiley and Sons: New York, 1988.

(6) Sly, K. L.; Nguyen, T. T.; Conboy, J. C. *Optics Express* **2012**, *20*, 21953.

(7) Hecht, E. *Optics*; Addison Wesley: San Francisco, 2002.

(8) Fowles, G. R. *Introduction to Modern Optics*; 2nd ed. ed.; Holt, Rinehart and Winston: New York, 1975.